

On the Accuracy of Fault Detection and Separation in Permanent Magnet Synchronous Machines using MCSA/MVSA and LDA

Reemon Z. Haddad, *Student Member, IEEE* and Elias G. Strangas, *Senior Member, IEEE*

Abstract—In this work the Motor Current/Voltage Signature Analysis and Linear Discriminant Analysis are evaluated with respect to the accuracy to detect the status of Permanent Magnet Synchronous Machines whether it is healthy or faulted, determine the type of that fault, and estimate the severity in the case of static eccentricity or turn-to-turn short circuit fault. Three types of faults are discussed: static eccentricity, turn-to-turn short circuit, and partial demagnetization fault. Two dimensional (2-D) Finite Element Analysis is used to model and simulate the machine under healthy and faulted conditions. Fast Fourier Transform is applied to the phase voltage or current signals to obtain the frequency spectrum. A combination of the amplitude of the harmonics of the stator voltage or current signals are used as detailed features for the classifier for fault detection. Linear Discriminant Analysis is chosen as a classification method for both, detecting the fault and estimate its severity. Two different winding types of Permanent Magnet Synchronous Machines are tested: a concentrated and a distributed winding machine. To validate the simulation results, experiments at different operational points are carried out and the results are compared with the Finite Element Analysis.

Index Terms—Demagnetization, Fast Fourier Transform, Eccentricity, Turn-to-turn short circuit, Linear discriminant analysis classification, Permanent magnet synchronous machine.

I. INTRODUCTION

PERMANENT magnet synchronous machines (PMSMs) play a major role in many industrial applications because of their high efficiency, reliability, wide operating range, and high torque density. These applications include traction power steering in electric/hybrid vehicles, robotics, and wind generation. Detecting a fault and the type of that fault in PMSMs is important, since each fault requires different mitigation action (either interruption in the operation or change in the controller) and in some cases, these actions can be opposite.

Many methods have been used to detect the type of fault in PMSMs and estimate its severity. These methods can be categorized as: time domain methods, frequency analysis methods as in [1]–[5], and time scale analysis methods such as Discrete or Continuous Wavelet Transform (D/CWT) [6], [7]. The Motor Current Signature Analysis (MCSA) and the Motor Voltage Current Analysis (MVCA) are the most common online methods for single fault detection [1], [8]–[10], since they do not require any additional connections or hardware.

This work was partially funded by National Science Foundation grant ECCS1102316, and Jordan University of Science and Technology.

The authors are with the Department of Electrical and Computer Engineering, Michigan State University, East Lansing MI 48824 USA (e-mail: haddadre@msu.edu; strangas@egr.msu.edu)

They are performed by applying spectral or time-frequency analysis techniques, like Fast Fourier Transform (FFT), Short Time Fourier Transform (STFT), or D/CWT, to the stator current or voltage signal.

Methods have already been developed to distinguish between faults. In [11] and [12] the variation in the incremental inductance curve is used as an indicator to detect and distinguish between eccentricity, uniform demagnetization and short circuit fault. In [13], the side band harmonics of the machine current signals are used to distinguish between inter-turn short circuit and rotor dynamic eccentricity faults in a permanent magnet synchronous generator. This method is able to detect the fault type (dynamic eccentricity or inter-turn fault) but not the severity accurately. In [14] and [15] the spectrum of the stator current and voltage signals is used to distinguish between static eccentricity, dynamic eccentricity and broken magnet for low power PMSMs; both experiments and simulation are performed to validate the method. Based on that work, dynamic eccentricity can be detected from the stator current harmonics, which are given as the multiple of the stator synchronous frequency divided by the number of pole pairs. Static eccentricity can be detected based on the increase in the amplitude in the 7th harmonic of the stator current signal. Broken magnets can be detected based on estimating the total *d*-axis magnetic flux and comparing it to the baseline healthy case. The main drawback of this approach is that it requires different methods to detect each fault, and the detection of the fault severity is based on the amplitude of the harmonics only which is not always possible for noisy conditions. In [16], the induced voltage in a search coil is used to separate between three faults: short circuit, demagnetization and eccentricity faults. The main drawback of this method is that the use of a search coil for fault detection may not be always possible. In [17] both the stator current and the voltage signals are used to detect eccentricity fault using the sideband subharmonic. It is shown that if the controller has a high bandwidth, the sideband subharmonic in the stator current signals will also appear in the commanded voltages.

Most of the detection methods in the literature like the MCSA and Linear Discriminant Analysis (LDA) have been used before for single fault detection. This approach is based on analyzing the stator current signal under healthy and faulted conditions. The appearance of the subharmonics can be used to detect the fault type and the subharmonics amplitude is used to estimate the severity.

The use of the subharmonics for fault detection presents

some difficulties. It is shown in [1] and [6] that similar side band patterns appear for both faults, eccentricity and short circuit fault. Also, the amplitudes of the generated subharmonics depend on the operating speed and load conditions. For non-stationary operation at lower speeds it is difficult to detect these sideband patterns [18]. In [19] and [20] it is shown that the relation between the number of poles and the stator slots affects the appearance of the subharmonics in the case of eccentricity faults. Based on this, using the subharmonics only for fault detection might not be adequate. However, there will always be a change in the amplitude of the harmonics of the voltage or current signals in a faulted machine.

The main contributions of this work include: 1) evaluating the accuracy of already existing methods, like the MCSA and the LDA to detect the machine status, whether it is healthy or faulted, separation between three different faults, and estimation of the fault severity. 2) Using either the measured stator currents or the commanded voltages for fault detection and identification. 3) Using the amplitude of the harmonics as fault detection and classification features instead of the subharmonics. Here, we continue the work of [3]. Three faults are tested: static eccentricity, demagnetization and turn-to-turn short circuit fault. Two machines with different winding topologies are tested using the proposed method. Simulation for the two machines, under healthy and faulted conditions is developed using two dimensional finite element analysis (FEA) software (FLUX-2D). The harmonics of the phase voltage/current are chosen as the features for the classifier. LDA is used as the classification method to detect the type of fault and estimate the severity. Experiments are conducted for both machines to validate the analysis and the simulation results.

Section II of this paper discusses the definition and the characteristics of the three different fault types. Section III gives the main parameters of the two tested machines, the experimental setup, and how faults are applied in finite element analysis and in the experiment. Section IV describes the main concept of LDA and how it is applied for fault detection and classification. Section V discusses LDA classification results for fault detection and estimation for both FEA and experimental data. In section VI Conclusions are drawn from the results.

II. CHARACTERISTIC OF THE FAULTS

Three faults are discussed and tested in this work: static eccentricity, demagnetization, and turn-to-turn short circuit fault. Each one of these faults develop in different ways and will cause different changes to the motor parameters and performance. Therefore, it is important to have a good understanding of each one of these faults, the characteristics, the causes and their effects.

A. Eccentricity fault

Eccentricity faults are the most common mechanical faults in electric machines. In a healthy machine, the air gap between the stator and the rotor is uniformly distributed. In a machine with eccentricity fault, the air gap is no longer uniform,

which leads to an asymmetric flux distribution, which in turn creates a radial force between the stator and the rotor. This force increases with eccentricity and has several effects: vibration, noise, and possibly wear of the bearings. This in time, may further increase the eccentricity and cause the rotor and the stator to rub. Therefore, detecting eccentricity faults and applying early maintenance while the fault is still in the early stage is very important to protect the machine from severe damage.

There are three different types of eccentricity. **Static eccentricity, (SE)**. In this fault the stator geometric axis center is different than that of the rotor and the rotation axis center. This may be caused by incorrect positioning during assembling of the machine or stresses applied to the machine stator. **Dynamic eccentricity (DE)**. In this fault, the rotor geometric axis center is different than that of the stator and the rotation axis center. The main reasons for dynamic eccentricity are a bent machine shaft, bearing wear, stresses applied to the shaft (e.g. thermal stresses) and mechanical resonance at critical speeds. **Mixed eccentricity, (ME)**. In this fault the rotation axis center is different than the stator and the rotor geometric axis center. Fig. 1 shows a comparison of the geometry between healthy machine and the three different eccentricity faults: static eccentricity, dynamic eccentricity and mixed eccentricity fault. Only static eccentricity is discussed and tested here because it is the most common type of eccentricity fault.

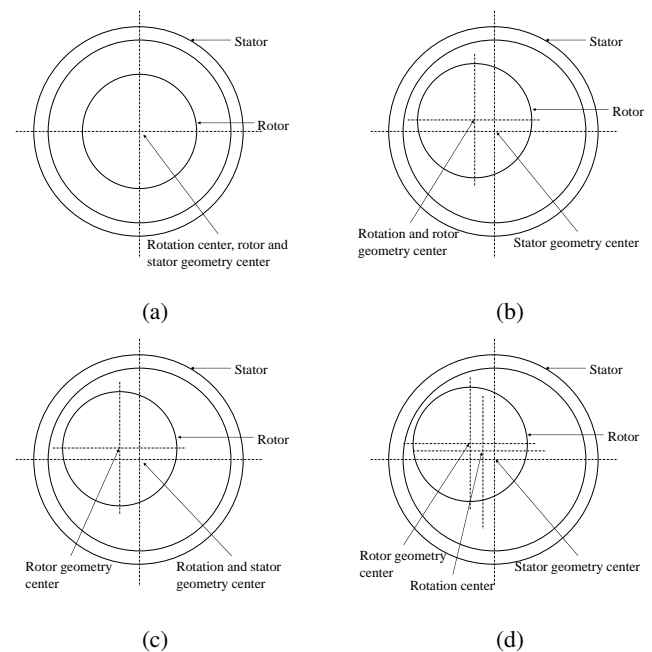


Fig. 1: (a) Healthy machine, (b) Static eccentricity, (c) Dynamic eccentricity, (e) Mixed eccentricity.

The severity of eccentricity fault is given by the following equation,

$$ECC = \frac{g_{max} - g_h}{g_h} \times 100\% \quad (1)$$

where ECC is the percentage of eccentricity fault severity, g_{max} is the maximum airgap in case of eccentricity fault, g_h is the machine airgap for healthy case. For healthy machine $g_{max} = g_h$ which means $ECC = 0\%$. According to [21], any eccentricity less than 10% can be neglected, and any eccentricity fault higher than 60% requires immediate repair to prevent any rubbing between the stator and the rotor, which damage the machine. Based on Fig. 2 and following [22], a general formula describing static eccentricity can be derived as follows:

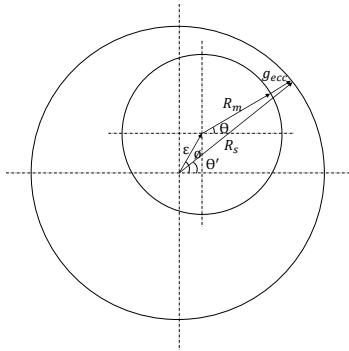


Fig. 2: Analytical approach to calculate eccentricity

$$R_s \cdot \cos(\theta') = \varepsilon \cos(\phi) + (R_m + g_{ecc}) \cos(\theta) \quad (2)$$

$$R_s \cdot \sin(\theta') = \varepsilon \sin(\phi) + (R_m + g_{ecc}) \sin(\theta) \quad (3)$$

where ε is the magnitude of the static eccentricity shift, ϕ is the angle of eccentricity shift and θ is the rotation angle. Taking the square of eqns. (2) and (3), and adding them together:

$$R_s^2 = \varepsilon^2 + (R_m + g_{ecc})^2 + 2\varepsilon(R_m + g_{ecc}) \cos(\phi - \theta) \quad (4)$$

$$\Rightarrow g_{ecc} = -\varepsilon \cos(\phi - \theta) \pm \sqrt{R_s^2 - \varepsilon^2 \sin^2(\phi - \theta)} - R_m \quad (5)$$

Since $R_s \gg \varepsilon$, the airgap in case of static eccentricity can be given as,

$$g_{ecc} = (R_s - R_m) - \varepsilon \cos(\phi - \theta) = g - \varepsilon \cos(\phi - \theta) \quad (6)$$

B. Turn-to-turn Short Circuit

Of the many possible types of stator winding faults, the turn-to-turn short circuit faults are the most common. A turn-to-turn fault can be due to mechanical, electrical and thermal stress in the stator winding. Stress may lead to an insulation breakdown of the coil conductor, which leads to shorting some of the turns. In this case, the shorted turns create an extra high-current path that is magnetically and electrically coupled with the winding current and a flux circuit path. This current heats the shorted turns, causing further insulation damage and may expand to nearby windings. Detecting the turn-to-turn fault at an early stage is important for protecting the machine winding from damage. Fig. 3 shows a series connected three phase winding with turn-to-turn short circuit fault at phase A. The fault is modeled by a small resistance R_f connected in parallel across the shorted turns.

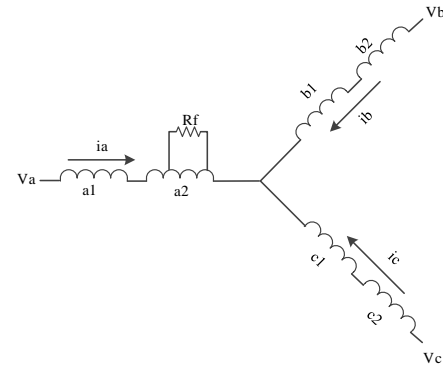


Fig. 3: Series winding with shorted turns.

C. Demagnetization

Demagnetization is also a common fault in PM machines. In these faults, the flux distribution in the machine is asymmetric and a high current flow in the windings. These currents weaken the insulation of the winding, increase the torque ripple and affect the machine performance and parameters. A main factor that might cause demagnetization faults is turn-to-turn short circuit fault, as the short circuit fault severity increases, this leads to demagnetized the rotor magnets. Therefore, it is important to detect the fault type and severity while it is still in the early stages. Other factors that might cause demagnetization fault include: aging of the magnet, high temperature, and operation under strong field weakening.

In this paper, LDA is used to detect the type of the fault and the severity based on the amplitude of the main harmonics of the current or voltage signals. Different LDA algorithms are used for fault detection in electrical machines [23]–[26]. In [23], LDA is used with discrete wavelet transform to choose the best wavelet filter to detect short circuit faults in induction machine. In [24] a comparison is made between different LDA algorithms: Classical LDA, Foley-Sammon LDA, and Uncorrelated LDA are used to detect reaction control system thruster faults in a launch vehicle. In [25], components from the vibration spectrum are used as features for LDA algorithm to detect bearing faults in induction machine.

III. FAULTS IMPLEMENTATION AND PROPOSED METHOD

Motors with different winding topologies create different stator current and voltage harmonics. Therefore, it is important to discuss the detection method for motors with different windings topologies. Two types of 3-phase PMSMs were modeled and tested. The first one has 16 poles and a concentrated winding distribution with 8 parallel branches per phase. The second has 12 poles and a distributed winding with 2 parallel branches per phase. Fig. 4(a) shows the geometric cross sectional area of the concentrated winding machine and Fig. 4(b) shows the cross section of the distributed winding machine. The specifications and parameters of the two machines are summarized in Table I.

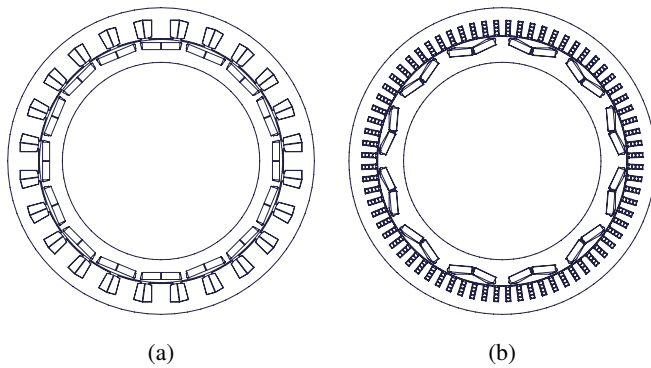


Fig. 4: Cross section for the two tested machines. (a) Concentrated winding machine. (b) Distributed winding machine

TABLE I: Parameters for the two tested machines

	Concentrated winding	Distribution winding
Number of phases	3 phase	3 phase
Maximum current	300A	300A
Maximum torque	310N.m	315N.m
Number of slots	24	48
Number of poles	16	12
Turns per phase	46	8

A. Finite Element Analysis

To model static eccentricity fault in FEA, the axis for the stator geometry should be different than that for both the rotor geometry and the rotational axis center. To do this, a separate coordinate system was assigned to the stator, different than the rotor and the rotated coordinate system; by changing the stator coordinate center, the stator axis geometry will only change. This allows controlling the direction and the degree of eccentricity without affecting the rotor geometric axis or the rotation center axis.

To simulate partial demagnetization using FEA, a new material with lower remanence value was assigned to replace the magnet and represent partial demagnetization. To model turn-to-turn short circuit fault for the concentrated winding machine, a new region was created in the winding slot. This region represents the short fault; the number of shorted turns was assigned to that region and subtracted from the original slot. A change was also made to the circuit model by adding a new coil conductor corresponding to the new faulted region. To represent this fault in the circuit, a resistance was connected in parallel across the new faulted coil conductor. To simulate turn-to-turn short circuit fault for the distributed winding machine, two end turns were shorted, this implied assigning all the shorted conductors to the short circuit coil in the circuit. Shorting two end turns corresponds to shorting of 12% of the total phase conductors. Another two end turns were shorted to represent a second severity of short circuit fault (25% of the total phase conductors were shorted).

B. Experimental Setup

National Instrument (NI) Real Time LabVIEW (RTL) was used to operate and control the machines. This real time

system consists of two desktop computers: one used as host and the other as the target. The controller was developed first in the host computer, then deployed to the target, where it was ran by the target computer's processor. The host computer was used to monitor data from the target and apply the changes to the controller parameters. A 100kW surface PMAC machine operated in a constant speed mode was used as a dynamometer.

Two faults were applied to the distributed winding machine experimentally: static eccentricity with two severity levels (25% and 50%), and two severity of short circuit fault (12% and 25% of phase A conductors were shorted). To apply static eccentricity fault, shims were mounted below the machine bearing to lift the rotor, as shown in Fig. 5. The same method was applied to the concentrated winding machine. To apply turn-to-turn short circuit fault, two turns of the machine windings were shorted through a resistance with a value of 0.125Ω , which is equivalent to 125% of the stator winding resistance. Another two turns were shorted to represent the second severity. Fig. 6 shows the the distributed winding machine with turn-to-turn short circuit fault implemented experimentally.

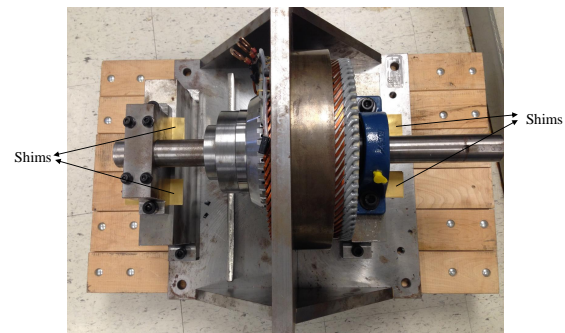


Fig. 5: Implementing eccentricity fault experimentally

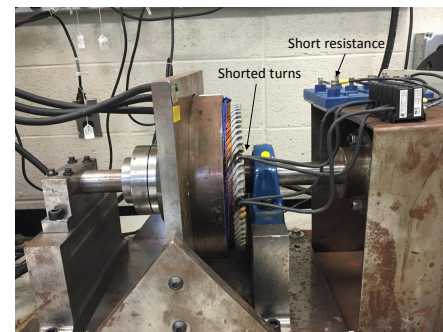


Fig. 6: Implementing short circuit fault experimentally

C. Algorithm for fault detection and classification

Fig. 7 shows the general flow diagram for the algorithm. The algorithm uses two classifiers: the first classifier detects the presence and type of the fault, while the second estimates the fault severity, once the type of fault was determined. The proposed method works as follows:

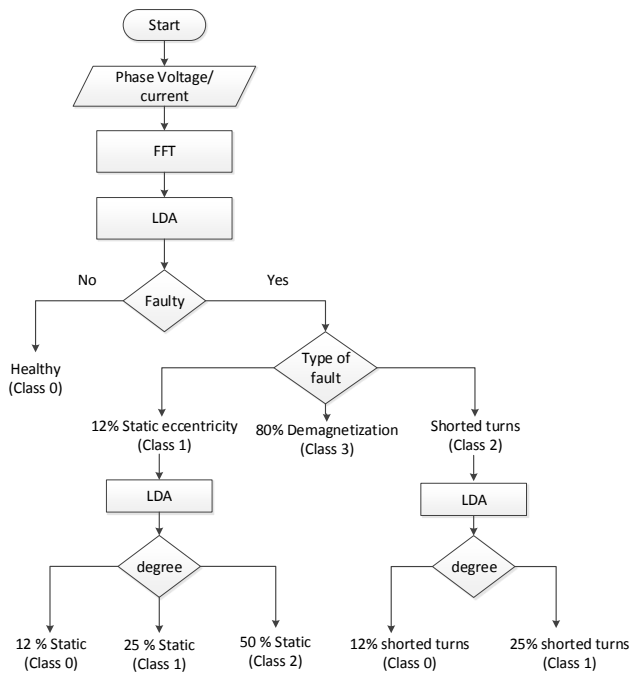


Fig. 7: Generalized flow chart for fault detection and identification

- [1] Three phase currents were used to control and operate the machine under both healthy and faulted conditions. The stator phase current or voltage signals in the abc frame of reference were measured for processing.
- [2] FFT was applied to the measured current or voltage signals. The amplitudes of the harmonics were selected as features for the classification. In this method a vector of the amplitude of the first 15 harmonics was chosen from phase A spectrum, as the features for each sample. (i.e. The fundamental and the harmonics 2^{nd} - 15^{th})
- [3] LDA classification is applied to detect whether the machine is healthy or faulted, and detect the type of the fault. The sample space for the first classifier contains samples from all studied faults. In the faulted case, it detects the type as one of the following: static eccentricity, turn-to-turn short circuit, or partial demagnetization.
- [4] If the fault was detected as static eccentricity or turn-to-turn short circuit fault, another LDA classifier was applied to detect the severity of that fault. In this classifier, the sample space contains samples from the same type of fault but with different severities.

IV. LINEAR DISCRIMINANT ANALYSIS (LDA)

LDA [27] is used to maximize the ratio between the variance for different classes and the variance within the same class, in order to achieve maximum separation between the feature sets in each class. For LDA, the sample space is divided into K classes, where each class consists of a specific number of samples corresponding to the same state. These classes are associated with weighting coefficients. These coefficients are used to calculate the corresponding linear discriminant

function for that class. The linear discriminant function for class k is given by (7):

$$C_k(X_i) = \alpha_{1k}x_{i1} + \alpha_{2k}x_{i2} + \dots + \alpha_{Nk}x_{iN} + \alpha_{N+1k} \quad (7)$$

where $X_i = [x_{i1}, x_{i2}, \dots, x_{iN}]$ is the N dimensional vector for the sample X_i , and $[\alpha_{1k}, \alpha_{2k} \dots \alpha_{N+1k}]$ is the coefficient matrix for the k^{th} class.

During the training phase, the weighting coefficient matrices are determined in an iterative process. Starting from arbitrary guesses of the $k \times N$ matrix, the weighting coefficient matrix is adjusted with each iteration. For each training sample X_i , its class k is known, and the coefficients are adjusted so that $C'_k(X_i)$ is greater for k than for all the other classes.

Once the training process is completed and the matrix C has been obtained, to classify an unknown sample, the coefficients computed during the training phase are used to calculate the discriminant functions for this sample. A sample vector belongs to a particular class if the linear discriminant function for that sample is greater than any other linear discernment function. A sample vector i belongs to a class j if:

$$C_j(X_i) \geq C_k(X_i) \quad \forall j \neq k \quad (8)$$

In this work, more than 15 samples were collected for different operating condition (current and speed), to determine the coefficient matrix. By varying the operating conditions, the coefficient matrix as function of current and speed is established for each class. For any test point not used in the training phase, the associated coefficients are obtained from the interpolation of the trained coefficient matrix. The resultant coefficients from each class are used to compute the class for fault detection and classification.

V. SIMULATION AND EXPERIMENTAL RESULTS

Field Oriented Control (FOC), as shown in Fig. 8, is used for the operation of the machine. The commanded currents i_d^* and i_q^* are subtracted from the measured currents i_d and i_q , then through a PI controllers, generate the commanded voltages v_d^* and v_q^* , which are used to control the machine. The harmonics of the measured currents are used as features for the LDA classifier. LDA can detect the type and the severity of the fault, based on the different variation in the amplitude of the harmonics caused by the different faults. It makes no difference if the harmonics of the voltages or the measured current signal are used for the classification. The commanded voltages are generated through PI controllers with a large bandwidth, so the harmonics that appear in the measured current signal, will also appear in the commanded voltages. It was proven in [17] that for a controller with higher bandwidth, the fault information produced in the current will also be contained in the voltage signal. Having a voltage sensor during the normal operation of the machine is not always necessary, while the measured feedback currents are always available.

Fig. 9 shows the spectrum of the stator current (phase A) for the distributed winding machine for the healthy case and for two faults with different severities (25% and 50% of eccentricity fault, 12% and 25% of the coils in phase A

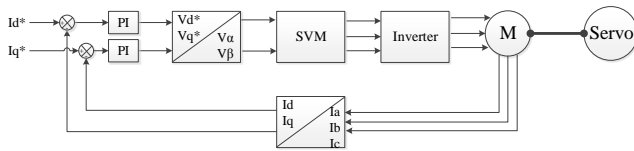


Fig. 8: Field Oriented Control block diagram

shorted). Fig. 10 shows the spectrum of the stator current (phase A) of the concentrated winding machine under healthy and two severities of eccentricity faults (25% and 50%). The current spectrum was collected with a current of 50A and operating speed of 500rpm. The amplitudes of the 5th and 7th harmonics are shown as an example for the change in the harmonics amplitude for faulted machine.

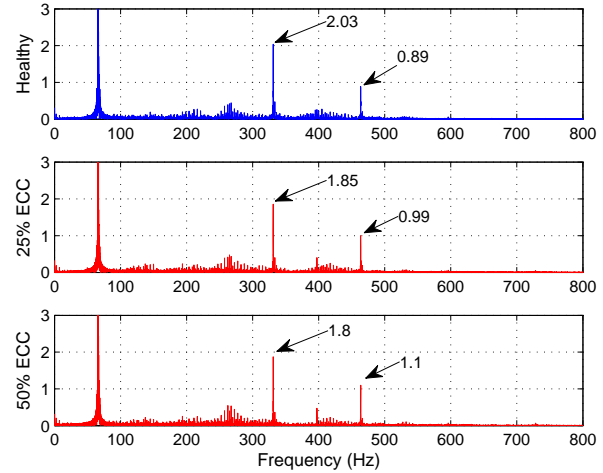


Fig. 10: Experimental results for the stator current frequency spectrum when healthy and eccentricity fault.

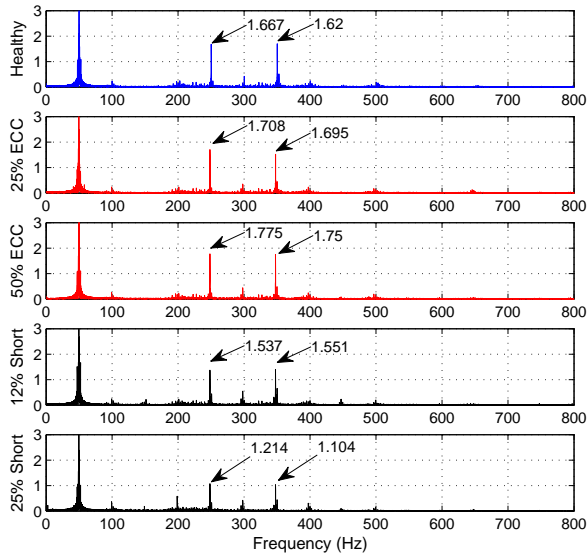


Fig. 9: Experimental results of the stator current spectrum for the distributed winding machine when healthy, eccentricity fault and short circuit fault.

It can be noticed from the harmonic spectrum that the appearance of the fault causes changes to the current (or voltage) spectrum. The relative change depends on the type and the severity of that fault. These changes in the main harmonics amplitude can be used as classification features to detect the fault type and estimate the severity.

A. Identifying the fault type

LDA classification was used first to detect the type of fault (static eccentricity, turn-to-turn short circuit, or demagnetization). Since the first 15 harmonics are used as features for the classifier, more than 15 samples are needed in the sample space for the LDA classification matrix to converge [28]. Table II shows the classification results of fault detection for both machines using FEA simulation for two different loads, LDA was performed separately at each load. The sample space

contains 44 samples that correspond to four different classes. Each class represents a specific machine state as follows: class 0 corresponds to the healthy case, class 1 corresponds to 12% static eccentricity, class 2 corresponds to 12% shorted conductors and class 3 corresponds to 80% demagnetization for one magnet. Each class contains 11 samples, generated by varying the speed from 1000 rpm to 2000 rpm in steps of 100 rpm. Two different operating loads were tested, 30% and 60% of the full load. The samples for each fault were chosen as the minimum accepted severity, so that, if the algorithm was able to detect the fault with lower severity, the fault with a higher severity can also be detected.

To validate the classification method the leave-one-out method is used; one sample from the sample space is selected and left out. The coefficient matrix is calculated from the rest of the samples. The selected sample is classified using these coefficients. This process is then repeated for every sample in the sample space. Each time the coefficients are recalculated and the left-out sample is classified using these coefficients. The classification accuracy for each class can be calculated as:

$$CC(\%) = \frac{N_{correct}}{N_{total}} \times 100\% \quad (9)$$

where $CC(\%)$ represents the percentage of the correct classification for each class, $N_{correct}$ is the number of the samples that are classified correctly and N_{total} is the total number of samples in the sample space. From the results in TableII, it can be noted that LDA is able to classify the type of fault correctly and distinguish between different faults for both machines at different operating conditions.

B. Identifying the fault severity

After detecting the fault and determining its type, it is necessary to estimate the severity. LDA was used again to estimate the severity of the eccentricity fault or the turn-to-turn short circuit fault. Table III shows the classification results for eccentricity severities for both machines under two different

TABLE II: LDA classification results for fault detection using FEA results. (11 samples/class, speeds 1000 – 2000 rpm).

	Correct classification			
	Concentrated Winding		Distribution Winding	
	30% full load	60% full load	30% full load	60% full load
Healthy	100%	100%	100%	91%
12% ECC	91%	91%	100%	91%
12% Short	100%	100%	100%	100%
80% Demag.	100%	100%	100%	100%

loads at 30% and 60% of full load using FEA simulation. Table IV shows the classification results for the turn-to-turn short circuit fault for both machines. For the static eccentricity case, the sample space consists of 33 samples for three different severities: 12%, 25%, and 45%. Each sample corresponds to a specific speed from 1000 rpm to 2000 rpm in steps of 100 rpm. A total of 3 classes assigned as follows: class 0 corresponds to 12% static eccentricity, class 1 corresponds to 25% static eccentricity and class 2 corresponds to 45% static eccentricity. For the turn-to-turn circuit fault, the sample space consists of 33 samples, corresponding to healthy case and two degrees of shorted turns: class 0 corresponds to healthy case, class 1 corresponds to 12% shorted conductors and class 2 corresponds to 25% shorted conductors. The leave-one-out method is used to validate the results.

TABLE III: LDA classification results to detect the severity of static eccentricity fault using FEA results. (11 samples/class, speeds 1000 – 2000 rpm).

	Correct classification			
	Concentrated Winding		Distribution Winding	
	30% full load	60% full load	30% full load	60% full load
12% ECC	91%	100%	100%	91%
25% ECC	91%	100%	100%	100%
45% ECC	100%	100%	100%	100%

TABLE IV: LDA classification results to detect the severity of turn to turn short circuit fault using FEA results. (11 samples/class, speeds 1000 – 2000 rpm).

	Correct classification			
	Concentrated Winding		Distribution Winding	
	30% full load	60% full load	30% full load	60% full load
Healthy	100%	100%	100%	91%
12% Short	91%	100%	91%	100%
25% Short	100%	100%	100%	100%

From the classification results, it is clear that LDA was able to detect the type of fault and estimate its degree for both machines. However, some of the samples related to the 12% static eccentricity fault were not classified correctly, even though only simulation experiments were used that did not have measurement noise. The reason was that for low severities of eccentricity faults, most of the harmonic

amplitudes for the 12% eccentricity were close to those for the healthy machine; hence the LDA classification cannot distinguish between healthy and the 12% static eccentricity fault for a few samples.

C. Comparing FEA with experimental data

In this paper we combined the effects of both speed and torque to evaluate the accuracy of LDA classification for fault detection and identification. First, the training samples and the testing samples were collected from operation with the same torque level. Samples for healthy and faulted machine were collected from three torque levels (20A, 50A and 70A). For each class 11 samples generated by varying the speed from 500 rpm to 1000 rpm in steps of 50 rpm, with a sampling frequency of 10kHz (10000 points are recorded for each sample (1s)). The leave-one-out method was used to test and validate the classification method. (Results are shown in Tables V and VI for cases 1, 3 and 4).

To evaluate the validity of the method when the testing samples were different than the training samples, samples from two torque levels were tested (30A and 100A). The coefficients used for these two cases were interpolated from the calculated coefficients from 20A, 50A and 70A. Each class contains 11 samples generated by varying the speed from 500 rpm to 1000 rpm in steps of 50 rpm. (Results are shown in Tables V and VI for cases 2 and 5).

An additional case was tested when the testing samples and training samples were differ in both speed and torque. For this case, each class contains 11 samples. The testing samples were collected while the machine was operating at a torque of 30A by varying the speed from 525 rpm to 1025 rpm in steps of 50 rpm. The coefficients were interpolated from the calculated coefficients from 20A, 50A and 70A by varying the speed from 500 rpm to 1000 rpm in steps of 50 rpm. (Results are shown in Tables V and VI for case 6).

Table. V shows a comparison of the correct classification results for fault detection between the experimental and FEA simulation for the distributed winding machine under healthy, 25% eccentricity fault and 12% short circuit fault. Table VI shows a comparison of the correct classification results between the experimental and FEA simulation for the concentrated winding machine under healthy and two severities of eccentricity fault (25% and 50%). Table VII shows a comparison of the classification results for fault severity detection between the experimental and FEA simulation for the distributed winding machine under two severities of eccentricity fault (25% and 50%). Table VIII shows a comparison of the correct classification results for fault severity detection between the experimental and FEA simulation for the distributed winding machine under two severities of short circuit fault (12% and 25%).

The results show that the most accurate classification can be achieved when the testing and the training samples were collected from the same load. A minimum of 82% of the samples were classified correctly. Interpolation for the training samples can be used if the testing samples were collected from a load close to the training samples load, but the accuracy

TABLE V: Comparison of LDA classification results between experiments and FEA to detect the fault type for the distributed winding machine. (11 samples/class, speeds 500 – 1000 rpm).

case #	Correct classification					
	Experimental results			FEA results		
	H	25% ECC	12% Short	H	25% ECC	12% Short
1-20A	91%	91%	100%	100%	100%	100%
2-30A	82%	82%	82%	91%	82%	91%
3-50A	91%	82%	91%	91%	91%	100%
4-70A	91%	82%	82%	90%	82%	82%
5-100A	72%	63%	72%	82%	72%	82%
6-30A/Speed	-	-	-	91%	82%	82%

TABLE VI: Comparison of LDA classification results between experiments and FEA for the concentrated winding machine.(11 samples/class, speeds 500 – 1000 rpm).

case #	Correct classification					
	Experimental results			FEA results		
	H	25% ECC	12% Short	H	25% ECC	12% Short
1-20A	100%	91%	100%	100%	100%	100%
2-30A	82%	72%	82%	91%	82%	91%
3-50A	91%	82%	91%	91%	91%	91%
4-70A	91%	82%	91%	91%	91%	91%
5-100A	72%	72%	72%	72%	72%	82%
6-30A/speed	-	-	-	82%	72%	82%

TABLE VII: Comparison of LDA classification results between experiments and FEA to detect the fault severity for the distributed winding machine. (11 samples/class, speeds 500 – 1000 rpm).

case #	Correct classification					
	Experimental results			FEA results		
	H	25% ECC	50% ECC	H	25% ECC	50% ECC
1-20A	91%	91%	91%	100%	91%	100%
2-30A	82%	82%	82%	91%	82%	91%
3-50A	91%	82%	82%	91%	91%	91%
4-70A	82%	82%	82%	91%	82%	82%
5-100A	72%	62%	82%	82%	82%	82%

TABLE VIII: Comparison of LDA classification results between experiments and FEA to detect short circuit fault severity for the distributed winding machine. (11 samples/class, speeds 500 – 1000 rpm).

case #	Correct classification					
	Experimental results			FEA results		
	H	12% Short	25% Short	H	12% Short	25% Short
1-20A	91%	91%	91%	100%	100%	100%
2-30A	82%	82%	91%	91%	91%	91%
3-50A	91%	82%	82%	91%	91%	100%
4-70A	82%	82%	91%	91%	82%	91%
5-100A	72%	72%	82%	82%	82%	82%

correct classification of 62% in the case of 100A was achieved to detect eccentricity fault. A minimum percentage of 72% was achieved in the case of 30A for eccentricity fault detection.

To test the method over the operating range and not only at specific torques, the entire sampling space was modified to contain different torques and speeds. Tables IX and X show a comparison of the correct classification results between experimental data and FEA of fault detection and classification for the distributed winding machine. The sample space for each class contains 40 samples, so a total of 120 samples were used to generate the training matrix. The 40 samples correspond to 4 different currents, each case contains 10 samples that were generated by varying the speed from 550 rpm to 1000 rpm in steps of 50 rpm. The combination of the amplitude of the first 15 harmonics were used as the features for the LDA classification. Fig. 11 shows the full training matrix construction for the healthy case and two different faults. Fig. 12 shows the construction of the healthy portion of the full training matrix.

$$\left[\begin{array}{cccccc}
 x_{11} & x_{12} & x_{13} & \cdots & x_{115} \\
 \vdots & \vdots & \vdots & & \vdots \\
 x_{401} & x_{402} & x_{403} & \cdots & x_{4015} \\
 x_{411} & x_{412} & x_{413} & \cdots & x_{4115} \\
 \vdots & \vdots & \vdots & & \vdots \\
 x_{801} & x_{802} & x_{803} & \cdots & x_{8015} \\
 x_{811} & x_{812} & x_{813} & \cdots & x_{8115} \\
 \vdots & \vdots & \vdots & & \vdots \\
 x_{1201} & x_{1202} & x_{1203} & \cdots & x_{12015}
 \end{array} \right] \left. \begin{array}{l} \\ \\ \\ \\ \\ \\ \\ \\ \\ \end{array} \right\} \begin{array}{l} \text{Healthy} \\ \\ 25\% \text{ ECC.} \\ \\ 12\% \text{ short} \end{array}$$

Fig. 11: Full training matrix for healthy case and two faults (25% eccentricity and 12% turns of phase A shorted).

$$\text{H} \left\{ \left[\begin{array}{cccccc}
 x_{11} & x_{12} & x_{13} & \cdots & x_{115} \\
 \vdots & \vdots & \vdots & & \vdots \\
 x_{101} & x_{102} & x_{103} & \cdots & x_{1015} \\
 x_{111} & x_{112} & x_{113} & \cdots & x_{1115} \\
 \vdots & \vdots & \vdots & & \vdots \\
 x_{201} & x_{202} & x_{203} & \cdots & x_{2015} \\
 x_{211} & x_{212} & x_{213} & \cdots & x_{2115} \\
 \vdots & \vdots & \vdots & & \vdots \\
 x_{301} & x_{302} & x_{303} & \cdots & x_{3015} \\
 x_{311} & x_{312} & x_{313} & \cdots & x_{3115} \\
 \vdots & \vdots & \vdots & & \vdots \\
 x_{401} & x_{402} & x_{403} & \cdots & x_{4015}
 \end{array} \right] \right\} \begin{array}{l} 20A \\ \\ 30A \\ \\ 40A \\ \\ 50A \end{array}$$

Fig. 12: Training matrix for healthy case only.

decreases if the training samples were collected from loads that were too different from the testing samples loads. A minimum

The results show that the proposed method was able to detect the type of the fault and estimate the severity either by using the harmonics of the phase voltages or of the

TABLE IX: A comparison of LDA classification results to detect the fault type for the distributed winding machine between experiments and FEA using the full training matrix.

Correct classification			
	Exp. using current	Exp. using voltage	FEA Data
Healthy	87.5%	85%	95%
25% ECC	85%	80%	88%
12% Short	88%	85.5%	92.5%

TABLE X: A comparison of LDA classification results to detect the severity of eccentricity fault for the distributed winding machine between experiments and FEA using the full training matrix.

Correct classification			
	Exp. using current	Exp. using voltage	FEA Data
Healthy	85.5%	87.5%	91%
25% ECC	77.5%	80%	87.5%
50% ECC	80%	77.5%	90.5%

current signals. When the training and testing features were extracted from samples collected at different operating loads, the classification results were not as accurate as in the case when the samples were collected from the same operating torque. For fault detection, an average of 89.6% of the samples were classified correctly for the FEA samples, 81% of the total samples were classified correctly from the experimental data using the harmonics in the measured feedback current, and 81.6% were classified correctly based on the harmonics in the voltage signal.

In practical applications, tested machines might differ due to the variations in the manufacturing tolerance and material property. To evaluate the robustness of the detection methods, Additive White Gaussian Noise (AWGN) with different Signal to Noise Ratio (SNR) levels was added to the tested current samples. A comparison of the classification results for fault detection between experimental and FEA is shown in Table XI. For this case, the sample space contains of 30 samples corresponding to three classes: healthy, 25% static eccentricity and one turn-to-turn short circuit fault. Each class contains 10 samples generated by varying the speed from 550 rpm to 1000 rpm in steps of 50 rpm, with a sampling frequency of 10KHz for a current of 20A. It is noted that the change in the harmonics amplitude due to the noise affects the classification results, which makes the detection based on the harmonics amplitude not robust at high noise levels.

D. Effect of Temperature

The change in the operating temperature causes multiple changes to the stator current and voltage of PMSMs. The increase of the operating temperature causes an increase in the stator resistance and a decrease in the magnet remanence. The effect of temperature is modeled in FEA for both tested machines by changing the values of the stator resistance and the magnet remanence flux based on the following formulas:

$$R_s(T) = R_{s20}(1 + \alpha_R * (T - 20)) \quad (10)$$

TABLE XI: A comparison of LDA classification results for the distributed winding machine for different SNR levels.(10 samples/class, speeds 550 – 1000 rpm).

Correct classification						
SNR (dB)	Experimental results			FEA results		
	H	25% ECC	12% Short	H	25% ECC	12% Short
100	90%	80%	90%	100%	100%	90%
90	90%	80%	90%	100%	100%	90%
80	88%	83%	85%	95%	92%	88%
70	80%	75%	79%	90%	86%	82%
60	70%	65%	71%	80%	70%	76%

$$B_r(T) = B_{r20}(1 + \alpha_{Br} * (T - 20)) \quad (11)$$

where R_{s20} is the value of the stator resistance at $20^{\circ}C$, $\alpha_R = 0.00393$ is the temperature coefficient for the stator resistance, B_{r20} is the magnet permeance of the rotor magnet at $20^{\circ}C$, $\alpha_{Br} = -0.0011$ is the temperature coefficient for the magnet and T is the operating temperature.

Table XII shows the simulation results of fault classification for fault detection under different temperatures for both machines. The sample space contains 40 samples corresponding to 4 classes: Healthy, 12% static eccentricity, 12% short circuit fault and 80% demagnetization. Each class consists of 11 samples generated by varying the speed from 1000 rpm to 2000 rpm in a steps of 100 rpm. The training samples were collected at an operating load of 20A at a temperature of $20^{\circ}C$, while the testing samples were collected at a temperatures of $20^{\circ}C$, $70^{\circ}C$ and $150^{\circ}C$.

TABLE XII: LDA classification results for fault detection using FEA results. (11 samples/class, speeds 1000–2000 rpm).

Correct classification						
	Concentrated Winding			Distribution Winding		
	$20^{\circ}C$	$70^{\circ}C$	$120^{\circ}C$	$20^{\circ}C$	$70^{\circ}C$	$120^{\circ}C$
Healthy	100%	72%	63%	100%	72%	63%
12% ECC	91%	72%	55%	91%	72%	63%
12% Short	100%	81%	63%	100%	81%	72%
80% Demag.	100%	63%	55%	91%	55%	55%

It can be noticed that the temperature is an important factor that needs to be considered. If the training samples are collected from a temperature that is relatively close to the testing samples temperature (difference in temperature between testing and training samples below $40^{\circ}C$), the classifier is able to detect the fault type. If testing samples are collected from temperature that is $40^{\circ}C$ or more than the training samples, the accuracy of the classifier reduces. To account for temperature variation, samples from FEA can be used as a training samples. However, the mesh quality and the variation in the material parameters causes small differences between the actual model and the simulated model. These changes might affect the harmonics amplitude, and reduce the accuracy of the classification. Often in practice FEA results are adjusted using empirical factors. In this case, samples collected from FEA can be used as a training samples.

VI. CONCLUSIONS

In this paper, the MSCA and LDA classifiers were evaluated for accuracy for fault detection and estimation in PMSM. The amplitude of the harmonics of the phase voltage or stator current signals were used as features for the LDA classifier to detect the fault type and estimate its severity. Three faults were discussed: static eccentricity, turn-to-turn short circuit, and partial demagnetization fault. Tests were performed using FEA and validated using experimental data for two types of PMSMs: a 12 poles distributed winding machine and a 16 poles concentrated winding machine.

Most of the previous detection and separation methods are based on using the subharmonics of the stator current signal while the motor is operating at a specific speed and torque. For the proposed method, experimental and simulation classification results show that the variation in amplitude of the current or voltage harmonics due to the presence of a fault in the machine, can be used to detect the fault type and estimate the severity under different operating speeds and loads. The accuracy of the classification depends on the density of the training samples in the sample space. The highest classification accuracy is achieved when the training and the testing samples are collected from similar operating conditions. Interpolation for the training samples can also be used if the testing samples are collected from a different operating conditions than the training samples. The accuracy will decrease when the training samples are collected from an operating conditions that are too different from the testing samples (results shown in Tables II-XII).

The proposed method is valid for the machine at steady state operation. Since that only the first 15 harmonics are needed for the classifier, only few cycles are needed. It is also important to mention that the magnitude of the resistance of the short was relatively high. Therefore, the amplitudes of the harmonics from all the phases were close in the case of short circuit fault. This makes the method able to detect the short circuit fault no matter which phase the features were extracted from, but not able to detect the fault location (i.e. the shorted phase).

REFERENCES

- [1] B. Ebrahimi, J. Faiz, and M. Roshtkhari, "Static-, Dynamic-, and Mixed-Eccentricity Fault Diagnoses in Permanent-Magnet Synchronous Motors," *IEEE Trans. Ind. Electron.*, vol. 56, no. 11, pp. 4727–4739, Nov 2009.
- [2] J. Rosero, A. Espinosa, J. Cusido, J. Ortega, and L. Romeral, "Simulation and Fault Detection of Short Circuit Winding in a Permanent Magnet Synchronous Machine (PMSM) by means of Fourier and Wavelet Transform," in *2008. IMTC 2008. IEEE Instrumentation and Measurement Technology Conference Proceedings*, May 2008, pp. 411–416.
- [3] R. Haddad and E. Strangas, "Fault Detection and Classification in Permanent Magnet Synchronous Machines Using Fast Fourier Transform and Linear Discriminant Analysis," in *2013 9th IEEE International Symposium Diagnostics for Electric Machines, Power Electronics and Drives (SDEMPED)*, Aug 2013, pp. 99–104.
- [4] J. Rosero, J. Cusido, A. Garcia, J. Ortega, and L. Romeral, "Study on the Permanent Magnet Demagnetization Fault in Permanent Magnet Synchronous Machines," in *IEEE IECON 2006 - 32nd Annual Conference Industrial Electronics*, Nov 2006, pp. 879–884.
- [5] L. Hao, S. Nawrocki, and X. Tang, "Modeling & Analysis of Weld Short Faults of Bar-Wound Propulsion IPM Machine Part I: Turn Short," in *2011 IEEE Vehicle Power and Propulsion Conference (VPPC)*, Sept 2011, pp. 1–6.
- [6] J. Rosero, J. Romeral, J. Cusido, J. Ortega, and A. Garcia, "Fault Detection of Eccentricity and Bearing Damage in a PMSM by Means of Wavelet Transforms Decomposition of the Stator Current," in *2008. APEC 2008. Twenty-Third Annual IEEE Applied Power Electronics Conference and Exposition*, Feb 2008, pp. 111–116.
- [7] I. Georgakopoulos, E. Mitronikas, A. Safacas, and I. Tsoumas, "Detection of Eccentricity in Inverter-Fed Induction Machines using Wavelet Analysis of the Stator Current," in *2008. PESC 2008. IEEE Power Electronics Specialists Conference*, June 2008, pp. 487–492.
- [8] S. Rajagopalan, W. Roux, T. Habetler, and R. Harley, "Dynamic Eccentricity and Demagnetized Rotor Magnet Detection in Trapezoidal Flux (Brushless DC) Motors Operating Under Different Load Conditions," *IEEE Trans. Power Electron.*, vol. 22, no. 5, pp. 2061–2069, Sept 2007.
- [9] J. Rosero, J. Ortega, A. Gacia, and L. Romeral, "On-line condition monitoring technique for PMSM perated with eccentricity," in *2007. SDEMPED 2007. IEEE International Symposium Diagnostics for Electric Machines, Power Electronics and Drives*, Sept 2007, pp. 95–100.
- [10] B. Ebrahimi and J. Faiz, "Feature Extraction for Short-Circuit Fault Detection in Permanent-Magnet Synchronous Motors Using Stator-Current Monitoring," *IEEE Trans. Power Electron.*, vol. 25, no. 10, pp. 2673–2682, Oct 2010.
- [11] J. Hong, S. Park, D. Hyun, T. June Kang, S. B. Lee, C. Kral, and A. Haumer, "Detection and Classification of Rotor Demagnetization and Eccentricity Faults for PM Synchronous Motors," *IEEE Trans. Ind. Appl.*, vol. 48, no. 3, pp. 923–932, May 2012.
- [12] R. Z. Haddad and E. G. Strangas, "Detection of Static Eccentricity and Turn-to-turn Short Circuit Faults in Permanent Magnet Synchronous AC machines," in *2015 IEEE 10th International Symposium Diagnostics for Electrical Machines, Power Electronics and Drives (SDEMPED)*, Sept 2015, pp. 277–283.
- [13] X. Zhaoxia and F. Hongwei, "Stator Winding Inter-Turn Short Circuit and Rotor Eccentricity Diagnosis of Permanent Magnet Synchronous Generator," in *2011 International Conference Control, Automation and Systems Engineering (CASE)*, July 2011, pp. 1–4.
- [14] W. le Roux, R. Harley, and T. Habetler, "Detecting Rotor Faults in Low Power Permanent Magnet Synchronous Machines," *IEEE Trans. Power Electron.*, vol. 22, no. 1, pp. 322–328, Jan 2007.
- [15] R. G. H. W. le Roux and T. G. Habetler, "Rotor Fault Analysis of a Permanent Magnet Synchronous Machine," (*ICEM02*) in *Proc. 15th Int. Conf. Electron. Mach.*, August 2002.
- [16] Y. Da, X. Shi, and M. Krishnamurthy, "A New Approach to Fault Diagnostics for Permanent Magnet Synchronous Machines Using Electromagnetic Signature Analysis," *IEEE Trans. Power Electron.*, vol. 28, no. 8, pp. 4104–4112, Aug 2013.
- [17] W. Le Roux, R. Harley, and T. Habetler, "Detecting Faults in Rotors of PM Drives," *IEEE Ind. Appl. Mag.*, vol. 14, no. 2, pp. 23–31, March 2008.
- [18] S. Rajagopalan, J. Aller, J. Restrepo, T. Habetler, and R. Harley, "Detection of Rotor Faults in Brushless DC Motors Operating Under Nonstationary Conditions," *IEEE Trans. Ind. Appl.*, vol. 42, no. 6, pp. 1464–1477, Nov 2006.
- [19] S. Nandi, S. Ahmed, and H. Toliyat, "Detection of Rotor Slot and Other Eccentricity Related Harmonics in a Three Phase Induction Motor with Different Rotor Cages," *IEEE Trans. Energy Convers.*, vol. 16, no. 3, pp. 253–260, Sep 2001.
- [20] Z. Zhu, L. Wu, and M. Mohd Jamil, "Influence of Pole and Slot Number Combinations on Cogging Torque in Permanent-Magnet Machines With Static and Rotating Eccentricities," *IEEE Trans. Ind. Appl.*, vol. 50, no. 5, pp. 3265–3277, Sept 2014.
- [21] W. Thomson and A. Barbour, "On-line Current Monitoring and Application of a Finite Element Method to Predict the Level of Static Airgap Eccentricity in Three-phase Induction Motors," *IEEE Trans. Energy Convers.*, vol. 13, no. 4, pp. 347–357, Dec 1998.
- [22] L. Cappelli, Y. Coia, F. Marignetti, and Z. Zhu, "Analysis of Eccentricity in Permanent-Magnet Tubular Machines," *IEEE Trans. Ind. Electron.*, vol. 61, no. 5, pp. 2208–2216, May 2014.
- [23] D. Asfani, S. Syafaruddin, M. Purnomo, and T. Hiyama, "Wavelet-LDA-Neural Network Based Short Circuit Occurrence Detection in Induction Motor Winding," in *2011 IEEE International Symposium Diagnostics for Electric Machines, Power Electronics Drives (SDEMPED)*, Sept 2011, pp. 330–336.
- [24] A. Krishnamurthy, M. Belur, and D. Chakraborty, "Comparison of Various Linear Discriminant Analysis Techniques for Fault Diagnosis of Re-usable Launch Vehicle," in *2011 50th IEEE Conference Decision and Control and European Control Conference (CDC-ECC)*, Dec 2011, pp. 3050–3055.

- [25] J. Harmouche, C. Delpha, and D. Diallo, "Linear Discriminant Analysis for the Discrimination of Faults in Bearing Balls by Using Spectral Features," in *2014 International Conference Green Energy*, March 2014, pp. 182–187.
- [26] R. Z. Haddad, C. A. Lopez, J. Pons-Llinares, J. Antonino-Daviu, and E. G. Strangas, "Outer Race Bearing Fault Detection in Induction Machines Using Stator Current Signals," in *2015 IEEE 13th International Conference Industrial Informatics (INDIN)*, July 2015, pp. 801–808.
- [27] T. Y. Young and T. W. Calvert, *Classification, Estimation and Pattern Recognition*. American Elsevier Publishing Co., 1974.
- [28] A. M. Martinez and A. Kak, "PCA versus LDA," *IEEE Trans. Pattern Anal. Mach. Intell.*, vol. 23, no. 2, pp. 228–233, Feb 2001.



Reemon Z. Haddad received the B.S. in Electrical Engineering from the Jordan University of Science and Technology, Jordan in 2010. He is currently working toward the Ph.D. degree in the Department of Electrical and Computer Engineering, Michigan State University, MI, USA. His research interests include the design and control of electrical machine and drives, and fault diagnosis and prognosis of permanent magnet synchronous machines.



Elias G. Strangas received the Dipl.Ing. degree in Electrical Engineering from the National Technical University of Greece, Athens, Greece, in 1975 and the Ph.D. degree from the University of Pittsburgh, Pittsburgh, PA. Since 1986, he has been with the Department of Electrical and Computer Engineering, Michigan State University, where he heads the Machines and Drives Laboratory. His research interests include the design and control of electrical machines and drives, finite-element methods for electromagnetic, and fault prognosis and mitigation

of electrical-drive systems.